STUDIES IN THE SYSTEM IRON OXIDE-TITANIUM OXIDE*

J. B. MacChesney† and Arnulf Muan, *The Pennsylvania State University, University Park, Pennsylvania*

Abstract

Phase equilibria in the system iron oxide-TiO_2 in air have been investigated at temperatures extending from the liquidus to slightly below the solidus. Stability relations among the phases spinel solid solution ($FeO \cdot Fe_2O_3$-$2FeO \cdot TiO_2$), hematite solid solution (Fe_2O_3-$FeO \cdot TiO_2$), pseudobrookite solid solution ($Fe_2O_3 \cdot TiO_2$-$FeO \cdot 2TiO_2$), rutile solid solution, liquid and gas are illustrated in an *apparently* binary diagram obtained by projecting ternary phase relations in the system FeO-Fe_2O_3-TiO_2 into the the join $FeO \cdot Fe_2O_3$-TiO_2.

Introduction

Titanium is relatively abundant in the earth's crust; igneous rocks contain an average of approximately 0.64 wt.% of this element. The most important titanium minerals are ilmenite ($FeO \cdot TiO_2$), titaniferous magnetite ($FeO \cdot Fe_2O_3$-$2FeO \cdot TiO_2$), rutile (TiO_2) and sphene ($CaO \cdot TiO_2 \cdot SiO_2$). A great deal of interest has been shown in these lately, especially in ilmenite and the titaniferous magnetites, because of their relation to rock magnetism and their possible use in petrogenesis and geothermometry. These minerals will be important indicators of the environment at time of their formation as the very complicated phase relations in the system FeO-Fe_2O_3-TiO_2 become better understood. Studies of this system will be most useful when completed for an extensive range of both temperature and O_2 partial pressure. In the present investigation a start on the broad study has been made by examining equilibrium relations in a region of relatively high temperature and O_2 partial pressure.

In previous papers emanating from this laboratory (Muan, 1955, 1958; Muan and Osborn, 1956) the special difficulties involved in studying high temperature phase equilibria in iron oxide containing systems have been pointed out. In all systems we have studied and described previously, iron was the only element present whose oxidation state was variable, while the others were noble gas type elements with constant oxidation state such as Si^{4+}, Al^{3+} and Mg^{9+}. In the case of the iron oxide-TiO_2 system, additional complications may arise because Ti also exists in different states of oxidation, viz. Ti^{4+}, Ti^{3+}, Ti^{2+}, and Ti^0. When attempting to study this system experimentally one should therefore keep the possibility in mind that Ti as well as Fe may undergo changes in oxidation states unless proper precautions are taken.
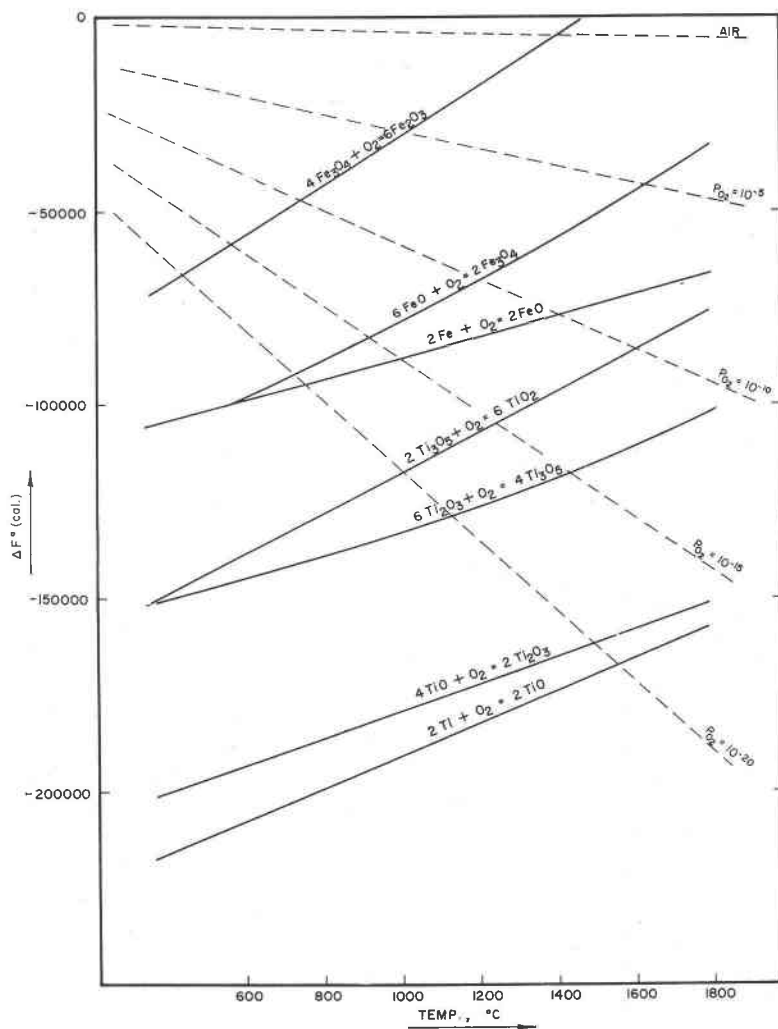
FIG. 1. Diagram showing standard free energy of formation of oxides of Fe and Ti as a function of temperature (solid lines). The curves have been constructed from thermodynamic data tabulated by Coughlin (1954). Dash curves indicate various levels of O_2 partial pressures as labeled in the diagram (0.21, 10^{-5}, 10^{-10}, 10^{-15}, 10^{-20} atm.).

In order to evaluate the relative stabilities of the various oxidation states of Ti and Fe it is instructive to examine a diagram showing standard free energies of formation of the various oxides of these elements as a function of temperature. Such a diagram is shown in Fig. 1, which has been constructed on the basis of data tabulated by Coughlin (1954). The

crystalline phases represented in the case of iron are Fe_2O_3 (hematite), $FeO \cdot Fe_2O_3$ (magnetite), "FeO" (wüstite) and Fe (metallic iron), while the crystalline phases encountered in the case of titanium are TiO_2 (rutile), Ti_3O_5, Ti_2O_3, TiO and Ti (metallic titanium). The $\Delta F°$ values for these reactions as labeled on the curves in the diagram all refer to 1 mol of oxygen. Hence the $\Delta F°$ values are related to the partial pressure of O_2 of the gas phase in equilibrium with condensed phases through the simple relation $\Delta F° = -RT \ lnK = RT \ ln \ p_{O2}$. Curves representing constant O_2 pressures of 0.21 (air), 10^{-5}, 10^{10}, 10^{-15} and 10^{-20} atm. are plotted as dash lines in Fig. 1. It is evident that the oxides of titanium are much more stable than those of iron. In the case of the pure substances, the lowest oxide of iron, "FeO," can be reduced to metallic iron at O_2 pressures which are still high enough to prevent the structure of the highest oxide of titanium, TiO_2 from decomposing to the structure of the next lower oxide, Ti_3O_5. In a liquid phase the restrictions on the valence states of the ions imposed by structural requirements are not critical, and continuous variations in the ratios of ions of different valences are possible. Hence the solid lines in the diagram of Fig. 1, pertaining to heterogeneous equilibria, would not be present in the case of a homogeneous liquid phase. The composition of the liquid, expressed in terms of Fe^{3+}/Fe^{2+} and Ti^{4+}/Ti^{2-*} ratios, would vary continuously as a function of temperature and O_2 partial pressure. Because of the much greater stability of the higher valence states of titanium than of iron, $\Delta F°$ for the reaction.

$$2 \ Fe^{3+}_{liq.} + Ti^{2+}_{liq.} = 2 \ Fe^{2+}_{liq.} + Ti^{4+}_{liq.}$$

would be strongly negative. From the relationship $\Delta F° = -RT \ ln \ K$, it is seen that K would be numerically very large and hence Ti^{4+}/Ti^{2+} very much higher than Fe^{3+}/Fe^{2+}. It is therefore to be expected that in a liquid made up from the oxides of titanium and iron the titanium will remain essentially as Ti^{4+} unless the Fe^{3+}/Fe^{2+} ratio is very low. Hence, only if extremely reducing conditions are imposed on the system in an attempt to obtain essentially all iron in the ferrous state is there seemingly any danger of reducing titanium to any appreciable extent to lower oxidation states than Ti^{4+}.

With the above considerations in mind we have chosen to start our study of iron oxide-titanium oxide equilibria by investigating the system in air ($p_{O_2} = 0.21$ atm.). In choosing to work at a constant O_2 pressure of this level we are studying a section through the system $Fe-Fe_2O_3-TiO_2$, which is part of the ternary system Fe-Ti-O. Methods for describing phase equilibria along an O_2 isobaric section through this system are anal-

---

* Ti^{4+} and Ti^{2+} are *chosen* as extreme valences of titanium in oxide phases. This choice does not rule out the possible existence of intermediate valence states such as Ti^{3+}; the latter corresponds formally to a mixture of Ti^{4+} and Ti^{2+} in the ratio 1:1.

ogous to those described for a large number of iron silicate systems, notably $FeO-Fe_2O_3-SiO_2$ (Muan, 1955). The most convenient presentation of phase relations is obtained by projecting the 0.21 atm. O_2 isobaric section into the join $FeO \cdot Fe_2O_3-TiO_2$. The diagram thus obtained has the appearance of a binary system, but the diagram can be used and interpreted correctly only if due consideration is given to its relation to the ternary system.

Previous Work

Several phase equilibrium studies in the pure iron oxide and pure titanium oxide systems have been reported in the literature. The most complete discussion of phase relations in the system Fe-O is found in the papers by Darken and Gurry in 1945 and 1946. A diagram summarizing some of their data which are particularly pertinent to our problem has been presented more recently by Muan (1958). The Ti-O system has attracted considerable interest in recent years. Andersson et al. (1957) are making very comprehensive studies of the phases present in this system. The data obtained by that group will serve to refine the approximate diagram for Ti-O inferred by DeVries and Roy (1954) on the basis of scattered data available in the literature.

Some of the general features of the ternary system $FeO-Fe_2O_3-TiO_2$ are fairly well established. Three solid solution series are known to exist in the system: the cubic magnetite-ulvospinel ($FeO \cdot Fe_2O_3-2FeO \cdot TiO_2$), the hexagonal hematite-ilmenite ($Fe_2O_3-FeO \cdot TiO_2$), and the orthorhombic pseudobrookite ($Fe_2O_3 \cdot TiO_2-FeO \cdot 2TiO_2$). In the first of these, magnetite-ulvospinel, a continuous solid solution exists at high temperatures, with exsolution taking place below 600° C. (Kawai, Kume, Sasajima, 1954; Vincent and Wright, 1957). The continuity of the hematite-ilmenite solid solutions seems to be in some doubt. Ramdohr (1926, 1950, 1953) reported that hematite and ilmenite form a continuous solid solution series above 600° C., while Pouillard (1950) found that two solid solution phases existed together in equilibrium at 950° C. These were described as $(Fe_{1-y}^{2+}Fe_{2y}^{3+}Ti_{1-y}^{4+}) O_3$ with $y = 1/3$ and $(Fe_{2-2x}^{3+}Fe_x^{2+}Ti_x^{4+}) O_3$ with $x = 1/3$, corresponding to a miscibility gap extending from approximately 33 to 67 mol%. Nicholls (1955) in a recent review states that it is well known from the work of Ramdohr (1926), as well as Posnjak and Barth (1934), that complete solid solubility exists between ilmenite and hematite above 1050° C. The value of 1050° C. apparently is confirmed by the work of Basta (1953) who showed the miscibility gap to be absent at this temperature.

The most recent and most comprehensive work on the pseudobrookite solid solution series is that of Akimoto and Nagata (1957). On the basis of sealed tube runs they reported a complete solid solution series between

$Fe_2O_3 \cdot TiO_2$ and $FeO \cdot 2TiO_2$ at 1200° C. Pouillard (1950), however, in his investigation of the system by a similar method could find no pseudo-brookite among the phases appearing at 950° C. Ramdohr (1950) reported that pseudobrookite grows at the expense of hematite-ilmenite solid solution at 1100° C., and Basta (1953) found that pseudobrookite appears as a new phase in magnetite-ilmenite intergrowths above 950° C. On the basis of these reports it seems reasonable to conclude that a lower temperature limit exists for the stability of pseudobrookite.

Another interesting feature of phase relations in the $FeO-Fe_2O_3-TiO_2$ system is the mutual solubility of ilmenite and magnetite solid solutions, which is thought to give rise to the intergrowths of magnetite-ulvospinel and ilmenite found in certain mineral deposits. The best evidence for the existence of this solid solution is afforded by Chevallier and Gerard (1950) who succeeded in producing a cubic solid solution crystal whose composition can be calculated as containing 37 mol% ilmenite. This is regarded by Nicholls (1955) as a solid solution not between the cubic and rhombohedral phases but between magnetite and metastable γ-$FeTiO_2$.

Reports on studies of phase relations close to the join $Fe_3O_4-TiO_2$ in the system $FeO-Fe_2O_3-TiO_2$ have appeared sporadically in the literature during the past 20 years. Junker (1936) made exploratory runs in air at liquidus temperatures with mixtures containing from 0 to 60 Wt.% iron oxide. He concluded tentatively that a "eutectic" exists at about 50 wt.% TiO_2. Ernst (1943) expanded the work, making runs in sealed tubes as well as in air. He identified the primary phase on the iron oxide side of the "eutectic" as pseudobrookite, which he believed to be stable at its melting point (approximately 1500° C.) and which he thought possessed considerable solubility for TiO_2 and limited solubility for FeO. Ernst also found evidence for the existence of a second "eutectic" between ilmenite-hematite solid solutions and pseudobrookite.

Experimental Method

General Procedure

The quenching technique was used in this study. Preheated mixtures of iron oxide and titanium oxide were held in platinum containers in air at constant temperature for a period of time sufficient to ensure equilibrium among gas, liquid and crystalline phases. These samples were then quenched rapidly to room temperature and the phases identified by microscopic and x-ray techniques. Compositions of liquids at liquidus temperatures were determined by chemical analysis of quenched samples.

Materials

Starting materials were reagent grade oxides ("Baker Analyzed"). After drying at 400° C for 18 hrs. the oxides were mixed in desired pro-

portions, ground under alcohol and fired to melting in a gas-air combustion furnace. These samples served as starting materials for runs of long duration for determination of subsolidus equilibria in the quench furnace, and occasionally also for quench runs in the liquidus temperature region. In most cases, however, samples from the gas-air furnace were heated in air at temperatures slightly above the expected liquidus temperature prior to determination of liquidus temperatures. This pretreatment of the mixtures ensured a close approach to the equilibrium $Fe_2O_3/$ FeO ratios of the samples and decreased the time necessary for equilibration runs in the quench furnace.

Platinum crucibles saturated with iron were used to contain the mixtures during prefiring in the gas-air furnace, and small envelopes made from thin platinum foil served as containers for samples during the quench runs. The use of platinum as material for containing iron oxide bearing samples does not cause any complications in studies carried out at relatively high levels of O_2 partial pressures, such as that of air $(p_{O_2} = 0.21$ atm.) used in the present investigation. For a more detailed discussion of this problem the reader is referred to a previous paper from this laboratory (Muan, 1957).

Furnaces and Temperature Control

The quenching experiments were carried out in vertical tube furnaces wound with platinum or platinum 20% rhodium resistance wire. Temperatures were measured before and after each run with a platinum: platinum-10% rhodium thermocouple calibrated at frequent intervals against standards with melting points defined as follows: $CaMgSi_2O_6$, 1391.5°; $CaSiO_3$, 1544° C. The temperatures given on this basis are in accordance both with the Geophysical Laboratory scale and with the 1948 International Scale (Corruccini, 1949; Sosman, 1952). Furnace temperatures were controlled by a second thermocouple inserted close to the heating element and connected through compensating lead wires to a Celetray controller.

Examination of Quenched Samples

Microscopic and x-ray methods were used for identification of phases present in the quenched samples. Examination of polished sections in reflected light was found more informative than examination in transmitted light under the petrographic microscope because of the opacity of most phases. The x-ray technique was used for determination of compositions of solid solution crystals, but could not be used as a tool for determination of liquidus temperatures because the liquids were exceedingly fluid and gave rise to formation of dendritic crystals even during the fastest quenching of the samples in mercury.

Divalent iron contents of samples quenched from liquidus tempera-
tures were determined by wet chemical analysis. The samples were
crushed in a Plattner mortar to pass a 100 mesh screen, after which
0.1–0.2 g. were heated to boiling in 20 ml. 1:3 H_2SO_4 in a covered
platinum crucible. When steam evolved, 5 ml. HF was added and the
solution was allowed to boil for 5–10 minutes. The crucible was then
plunged into a 600 ml beaker containing 5 vol.% H_2SO_4 saturated with
boric acid, and the solution was titrated with 0.05 n $KMnO_4$. No anal-
ysis for total iron oxide content was carried out. Previous experience
from similar studies in our laboratories (Muan and Gee, 1956; Muan,
1957; Phillips and Muan, 1958) has indicated that the loss of iron by
alloying in the thin platinum foil used as containers for the samples dur-
ing the equilibrium runs is negligible as long as the partial pressure of O_2
of the gas phase is as high as that of air. Furthermore, the platinum
crucibles used for pre-melting the starting mixtures in the more reducing
atmosphere of the gas-air combustion furnace were saturated with iron
under the conditions prevailing in this furnace through repeated previous
use.

RESULTS

Results of quenching experiments are summarized in Table I and
illustrated graphically in Fig. 2. Two diagrams are used in this figure in
order to show the phase relations as clearly as possible. The upper dia-
gram has the appearance of a binary system with $FeO \cdot Fe_2O_3$ and TiO_2
chosen as components. Stability ranges of the various phases as a func-
tion of temperature can be read directly off this diagram. However, be-
cause the FeO/Fe_2O_3 ratios in all phases present are not equal to 1:1
(molar basis) as in $FeO \cdot Fe_2O_3$, true compositions of condensed phases
cannot be represented in terms of the two chosen components. The
supplementary triangular diagram $FeO-Fe_2O_3-TiO_2$ in the lower half of
the figure is presented in order to show true compositions of condensed
phases. Because of the restrictions imposed by structural requirements,
the crystalline phase compositions will vary essentially along parts of
straight lines in this diagram, corresponding to binary solid solution
series. There are three such series in the system $FeO-Fe_2O_3-TiO_2$, indi-
cated by light straight lines in Fig. 2. One is the magnetite-ulvospinel
($FeO \cdot Fe_2O_3-2FeO \cdot TiO_2$) series of solid solution crystals with spinel
structure, the second is the series between hematite (Fe_2O_3) and ilmenite
($FeO \cdot TiO_2$) with hexagonal $\alpha-R_2O_3$ structure, and the third is the series
with pseudobrookite structure between the composition points Fe_2O_3
$\cdot TiO_2$ and $FeO \cdot 2TiO_2$.*

* In order to obtain experimently compositions throughout these solid solution series,
one has to either vary the O_2 partial pressure over wide limits or work with sealed contain-
ers.

TABLE I. RESULTS OF QUENCHING EXPERIMENTS

Temp. of Quenching Run (C °)	Phases Present*	Temp. of Run for Anal. (C °)	Initial Comp. (Wt. %)		Comp. after Equil. (Wt. %) (by analysis)		
			Fe₃O₄	TiO₂	FeO	Fe₂O₃	TiO₂

Temp. of Quenching Run (C °)	Phases Present*	Temp. of Run for Anal. (C °)	Initial Comp. (Wt. %)		Comp. after Equil. (Wt. %) (by analysis)		
			Fe_3O_4	TiO_2	FeO	Fe_2O_3	TiO_2
1555	Magn.(ss)		99	1			
1515	Magn.(ss)						
1477	Magn.(ss)+Hem.(ss)						
1555	Magn.(ss)+Liq.		98	2			
1515	Magn.(ss)+Hem.(ss)						
1477	Magn.(ss)+Hem.(ss)						
1571	Liq.		97	3			
1531	Magn.(ss)+Liq. (tr.)						
1520	Magn.(ss)+Hem.(ss) (tr.)						
1469	Magn.(ss)+Hem.(ss)						
1441	Magn.(ss)+Hem.(ss)						
1420	Hem.(ss)						
1562	Liq.	1,565	95	5	25.5	69.5	5.0
1554	Magn.(ss) (tr.) +Liq.						
1551	Magn.(ss) (tr.) +Liq.						
1547	Magn.(ss) (tr.) +Liq.						
1502	Magn.(ss)+Hem.(ss)						
1547	Liq.		93	7			
1542	Magn.(ss)+Liq.						
1524	Magn.(ss)+Liq.						
1516	Magn.(ss)+Hem.(ss)						
1504	Magn.(ss)+Hem.(ss)						
1468	Magn.(ss) (tr.)+Hem.(ss)						
1463	Hem.(ss)						
1529	Magn.(ss) (tr.) +Liq.		90	10			
1502	Magn.(ss) (tr.) +Hem.(ss)						
1470	Hem.(ss)						
1441	Hem.(ss)						
1529	Liq.	1,530	88	12	23.6	64.4	12.0
1520	Hem.(ss)+Liq. (tr.)						
1502	Hem.(ss)						
1470	Hem.(ss)						
1441	Hem.(ss)						

* Abbreviations used in this and succeeding tables have the following meanings: Liq. = liquid; Magn.(ss) = crystals of magnetite solid solution; Hem.(ss) = crystals of hematite solid solution; P. Brook.(ss) = crystals of pseudobrookite solid solution; Rut.(ss) = crystals of rutile solid solution; tr. = trace.

TABLE I (*continued*)

Temp. of Quenching Run (C °)	Phases Present*	Temp. of Run for Anal. (C °)	Initial Comp. (Wt. %)		Comp. after Equil. (Wt. %) (by analysis)		
			Fe_3O_4	TiO_2	FeO	Fe_2O_3	TiO_2
1534	Liq.		85	15			
1527	Liq.						
1520	Hem.(ss) (tr.) +Liq.						
1511	Hem.(ss)+Liq.						
1508	Hem.(ss)						
1470	Hem.(ss)						
1441	Hem.(ss)						
1513	Liq.	1,518	80	20	21.5	58.5	20.0
1511	Hem.(ss) (tr.) +Liq.						
1494	Hem.(ss)+Liq. (tr.)						
1486	Hem.(ss)+P. Brook.(ss)						
1470	Hem.(ss)+P. Brook.(ss)						
1441	Hem.(ss)+P. Brook.(ss)						
1500	Liq.		75	25			
1496	Hem.(ss)+Liq.						
1492	Hem.(ss)+P. Brook.(ss)						
1470	Hem.(ss)+P. Brook.(ss)						
1523	Liq.	1,530	70	30	18.3	51.7	30.0
1520	P. Brook.+Liq.						
1498	P. Brook.+Liq.						
1492	Hem.(ss)+P. Brook.(ss)						
1545	Liq.	1,545	65	35	20.4	44.6	35.0
1531	P. Brook.(ss)+Liq.						
1495	P. Brook.(ss)+Liq. (tr.)						
1492	P. Brook.(ss)+Hem.(ss) (tr.)						
1396	P. Brook.(ss)+Hem.(ss)						
1549	Liq.		62	38			
1534	P. Brook.(ss)+Liq.						
1524	P. Brook.(ss)+Liq.						
1504	P. Brook.(ss)+Liq. (tr.)						
1502	P. Brook.(ss)						
1486	P. Brook.(ss)						
1413	P. Brook.(ss)						
1555	Liq.		57.5	42.5			
1547	P. Brook.(ss)+Liq.						
1542	P. Brook.(ss)+Liq. (tr.)						
1531	P. Brook.(ss)						
1492	P. Brook.(ss)						
1551	Liq.		57.1	42.9			
1547	P. Brook.(ss) (tr.) +Liq.						

TABLE I (*continued*)

Temp. of Quenching Run (C °)	Phases Present*	Temp. of Run for Anal. (C °)	Initial Comp. (Wt. %)		Comp. after Equil (Wt. %) (by analysis)		
			Fe₃O₄	TiO₂	FeO	Fe₂O₃	TiO₂
1542	P. Brook.(ss)+Liq.						
1537	P. Brook.(ss)+Liq.						
1528	P. Brook.(ss)						
1492	P. Brook.(ss)						
1400	P. Brook.(ss)						
1553	Liq.	1,555	56.0	44.0	21.3	34.7	44.0
1542	P. Brook.(ss)						
1492	P. Brook.(ss)						
1400	P. Brook.(ss)						
1556	Liq.		54.0	46.0			
1546	P. Brook.(ss) (tr.) +Liq.						
1542	P. Brook.(ss)+Liq.						
1534	P. Brook.(ss)+Liq. (tr.)						
1492	P. Brook.(ss)						
1400	P. Brook.(ss)						
1556	Liq.	1,560	53	47	19.7	33.3	47.0
1549	P. Brook.(ss)+Liq.						
1531	P. Brook.(ss)+Liq. (tr.)						
1527	P. Brook.(ss)						
1400	P. Brook.(ss)						
1549	Liq.		50	50			
1543	Liq.						
1534	P. Brook.(ss)+Liq.						
1516	P. Brook.(ss)+Liq.						
1503	P. Brook.(ss)+Rut.(ss)						
1492	P. Brook.(ss)+Rut.(ss)						
1400	P. Brook.(ss)+Rut.(ss)						
1540	P. Brook.(ss) (tr.)+Liq.	1,545	48	52	18.7	29.3	52.0
1518	P. Brook.(ss)+Liq. (tr.)						
1490	P. Brook.(ss)+Rut.(ss)						
1400	P. Brook.(ss)+Rut.(ss)						
1534	Liq.		42	58			
1525	Liq.						
1520	P. Brook.(ss)+Liq.						
1517	P. Brook.(ss)+Rut.(ss)+Liq. (tr.)						
1511	P. Brook.(ss)+Rut.(ss)						
1552	Liq.	1,555	40	60	16.3	23.7	60.0
1542	Liq.						
1534	Rut.(ss) (tr.) +Liq.						
1517	Rut.(ss)+Liq.						

TABLE I (*continued*)

Temp of Quench-ing Run (C °)	Phases Present*	Temp. of Run for Anal. (C °)	Initial Comp. (Wt. %)		Comp. after Equil. (Wt. %) (by analysis)		
			Fe_3O_4	TiO_2	FeO	Fe_2O_3	TiO_2
1510	Rut.(ss)+P. Brook.(ss)						
1552	Rut.(ss) (tr.)+Liq.		39.5	61.5			
1552	Rut.(ss) (tr.) +Liq.		37.0	63.0			
1529	Rut.(ss)+Liq.						
1516	Rut.(ss)+P. Brook.(ss)						
1511	Rut.(ss)+P. Brook.(ss)						
1520	Rut.(ss)+Liq.		20.0	80.0			
1503	Rut.(ss)+P. Brook.(ss)						
1520	Rut.(ss)+Liq.		17.5	82.5			
1503	Rut.(ss)+P. Brook.(ss)						
1520	Rut.(ss)+Liq.		15.0	85.0			
1503	Rut.(ss)+P. Brook.(ss)						
1470	Rut.(ss)+P. Brook.(ss)						
1420	Rut.(ss)+P. Brook.(ss)						
1543	Rut.(ss).+Liq.		13.0	87.0			
1538	Rut.(ss)+Liq. (tr.)						
1510	Rut.(ss)						
1469	Rut.(ss)						
1420	Rut.(ss)+P. Brook.(ss) (tr.)						
1543	Rut.(ss)+Liq. (tr.)		10	90			
1510	Rut.(ss)						
1470	Rut.(ss)						
1420	Rut.(ss)						
1543	Rut.(ss)		7	93			
1509	Rut.(ss)						
1470	Rut.(ss)						
1420	Rut.(ss)						
1543	Rut.(ss)		5	95			
1505	Rut.(ss)						
1473	Rut.(ss)						
1420	Rut.(ss)						
1543	Rut.(ss)		3	97			
1420	Rut.(ss)						
1543	Rut.		0	100			
1500	Rut.						
1420	Rut.						

In contrast to these compositional variations of crystalline phases along essentially straight lines, the composition of the liquid at liquidus temperatures varies along the irregularly shaped dash curve in the lower diagram of Fig. 2. Light solid and dashed lines are conjugation lines connecting points representing approximate compositions of liquid and crystalline phases coexisting in equilibrium. In order to represent compositions in the upper "binary" diagram in terms of the chosen components $FeO \cdot Fe_2O_3$ and TiO_2, a method must be adopted for projecting true compositions represented by points in the ternary system on to this join. In accordance with previous practice (Muan and Gee, 1956; Muan, 1958, Phillips and Muan, 1958) we have projected all compositions along straight lines originating at the O corner of the triangle representing the Fe-Ti-O system. These straight lines are the "oxygen reaction lines" representing changes in total composition of condensed phases of mixtures as these react with oxygen of the atmosphere. For purposes of illustration consider the spinel phases designared respectively by a'' and f'' in the upper diagram (Fig. 2). Points a'' and f'' can be located on the lower diagram by the intersections of the dash-dot curves with the $FeO \cdot Fe_2O_3$-TiO_2 join. Proper projection of these points along the appropriate "oxygen reaction lines," which are very nearly parallel to the Fe_2O_3-FeO side of the composition triangle, allows estimation of the true compositions of the corresponding spinel phases. Point a'' is found to be the composition shown by the open circle at $FeO \cdot Fe_2O_3$, while the point corresponding to f'' lies further along the spinel solid solution join. The composition of the crystalline phases represented at the points g'', c'' and d'' of the upper diagram can be obtained by analogous methods.

The most notable features of the diagrams are as follows: Liquidus temperatures decrease as the first amounts of TiO_2 are added to iron oxide, from 1594° C. for pure iron oxide (Darken and Gurry, 1946) to 1524° C. in a mixture containing 12 wt.% TiO_2, with magnetite (ss) as the primary crystalline phase in this composition range. Hematite (ss) is the primary crystalline phase in the composition range 12–27 wt.% TiO_2, with liquidus temperatures decreasing from 1524 to 1493° C. A liquid of the latter TiO_2 content is in equilibrium with hematite (ss) as well as pseudobrookite (ss) at what appears as a eutectic situation at 1493° C. This is in reality a univariant situation corresponding to the intersection between the 0.21 atm. O_2 isobar and a ternary univariant line in the system FeO-Fe_2O_3-TiO_2 along which two crystalline phases coexist in equilibrium with a liquid and a gas phase. However, the existing degree of freedom has been "used up" in our choosing the O_2 partial pressure as that of air. As more TiO_2 is added to the mixtures, pseudobrookite is the primary crystalline phase, and liquidus temperatures
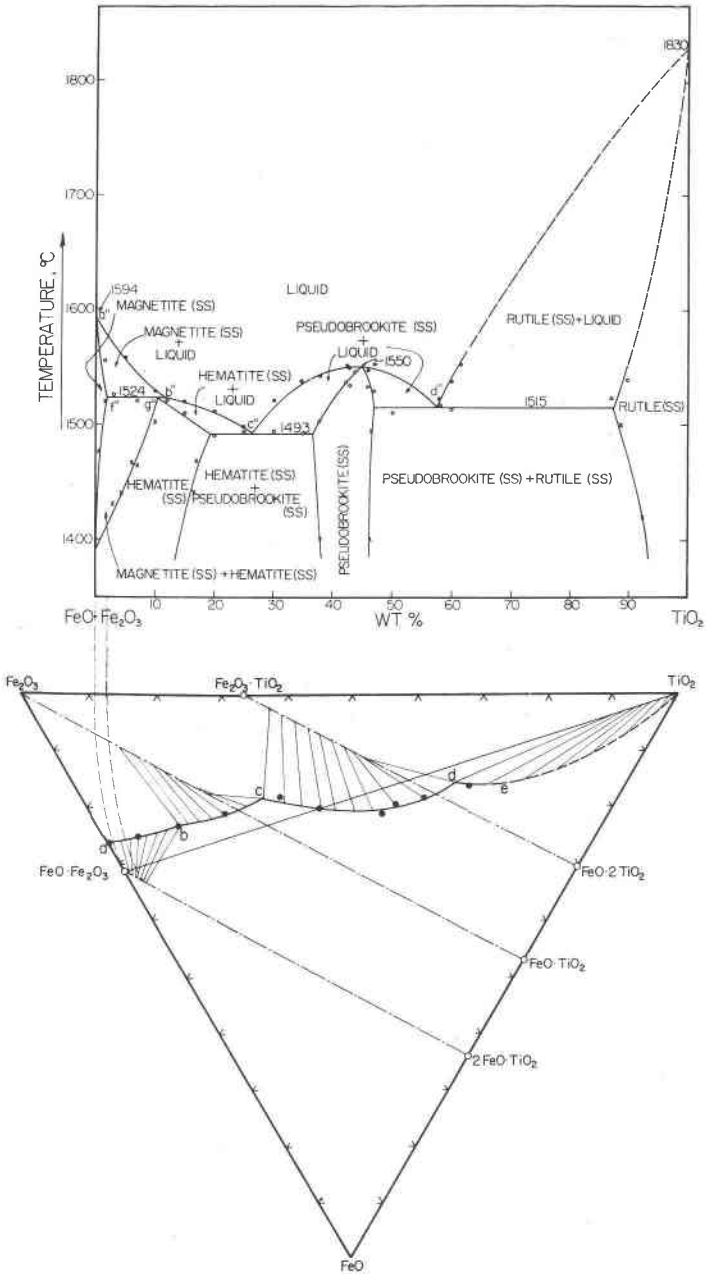
Fig. 2. Diagrams presented in order to show phase relations in the system iron oxide-TiO₂ in air. The upper half of the figure is a diagram with the appearance of a binary

increase. The liquidus curve goes through a maximum at approximately 1550° C. and 45 wt.% TiO_2, and subsequently decreases to another "eutectic," characterized by the coexistence at 1515° C. of the phases pseudobrookite (ss), rutile (ss), a liquid containing 58 wt.% TiO_2, and gas of O_2 partial pressure equal to 0.21 atm. With rutile as the primary crystalline phase, liquidus temperatures increase rapidly as the TiO_2 content is increased above 58 wt.%, reaching a maximum of approximately 1830° C. for the pure TiO_2 end member (the latter based on data summarized by DeVries and Roy, 1954).

The most notable feature of the subsolidus phase relations is the marked influence of TiO_2 on the equilibrium decomposition temperature of the sesquioxide (α-R_2O_3) structure of hematite to the spinel structure of magnetite. This decomposition temperature in air goes up from 1390° C. for the pure iron oxide end member to a maximum of 1524° C. as TiO_2 is added.

A summary of "invariant" situations in the system iron oxide-TiO_2 in air is presented in Table II, and x-ray diffraction data for pseudobrookite and rutile are listed in Table III.

DISCUSSION

One of the most interesting observations made in this investigation is that of the very strong stabilizing influence of TiO_2 on the hexagonal α-R_2O_3 structure of hematite relative to the spinel structure of magnetite. The addition of as little as 10 wt.% TiO_2 to iron oxide raises the temperature of the hematite to magnetite decomposition from 1390° C. to 1524° C. in air. This observation is important for an understanding of stability relations existing among iron oxide-TiO_2 minerals and may also have some important implications in technology. The change back and forth from one of these structures to the other in response to changes in temperature or O_2 partial pressure or both has been recognized in recent

system, showing the phases present as a function of temperature. Heavy lines are boundary curves. Solid dots, open circles and crosses represent experimentally determined points on liquidus, solidus and subsolidus boundary curves, respectively, based on data contained in Table I. The lower, triangular diagram shows compositions of crystalline and liquid phases. The heavy dash curve *a b c d e* represents compositions of liquids along the liquidus surface in air. Crystalline phases have compositions approximately represented by parts of the joins $FeO \cdot Fe_2O_3$-$2FeO \cdot TiO_2$, Fe_2O_3-$FeO \cdot TiO_2$ and $Fe_2O_3 \cdot TiO_2$-$FeO \cdot 2TiO_2$. Solid circles represent compositions of liquids as determined by chemical analysis. Light solid and dash lines are approximate locations of conjugation lines connecting points representing compositions of liquid and crystalline phases existing together in equilibrium in air. Light dash-dot and dash-double dot lines are auxiliary construction lines as explained in the text.

TABLE II. SUMMARY OF "INVARIANT"* SITUATIONS IN THE SYSTEM
IRON OXIDE-TiO_2 IN AIR

Phases Present	Comp. of Liquid (Wt. %)			Temperature (° C)
	FeO	Fe_2O_3	TiO_2	
Magn.+Liq.	27	73	0	1,594
Magn.+Hem.	27	73	0	1,390
Magn.(ss)+Hem.(ss)+Liq.	23	65	12	1,524
Hem.(ss)+P. Brook.(ss)+Liq.	18	55	27	1,493
P. Brook.(ss)+Liq.	20	35	45	1,550
P. Brook.(ss)+Rut.(ss)+Liq.	16	26	58	1,515
Rut.+Liq.	0	0	100	1,830

* The phase assemblages listed in reality represent univariant situations in the ternary system Fe-Ti-O. However, the existing degree of freedom has been "used up" in choosing the O_2 partial pressure of the gas phase, and hence the situations may be considered "invariant."

years as an important cause of damage to refractories used in steelmaking furnaces (see for instance a paper by Osborn, 1956). The stabilization of the hematite structure relative to that of magnetite, caused by TiO_2, may be advantageous or disadvantageous as far as refractories behavior

TABLE III. POWDER X-RAY DIFFRACTION DATA FOR PSEUDO-
BROOKITE AND RUTILE Fe K_α RADIATION

Pseudobrookite		Rutile	
(57.1 Wt. % Iron Oxide, 42.9 Wt. % TiO_2)		(TiO_2)	
d-Spacing	Intensity*	d-Spacing	Intensity*
4.92	W	3.25	S
3.49	S	2.49	W
2.75	S		
2.46	W	2.19	W
2.41	W	1.69	M
2.23	W	1.63	M
2.20	W		
1.97	M		
1.87	M		
1.76	W		
1.67	W		
1.64	W		
1.55	W		

* Abbreviations used have the following meanings: S=strong; M=medium; W=weak.

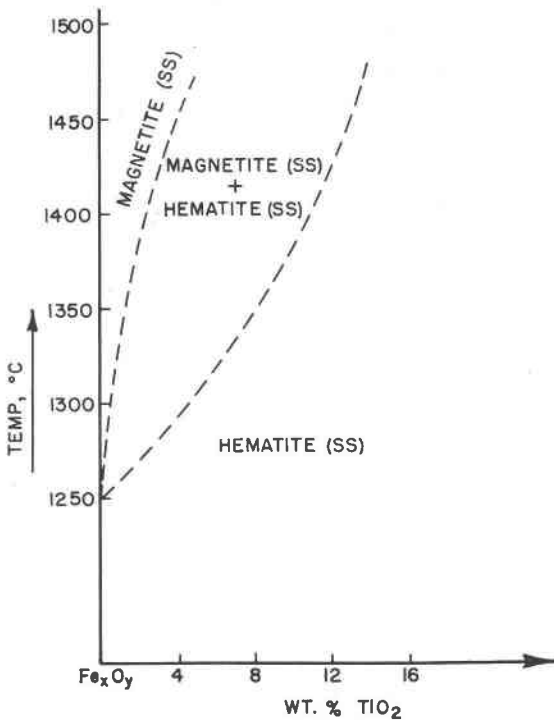FIG. 3. Sketch presented in order to show approximate stability relations among sesquioxide and spinel phases in system iron oxide-TiO$_2$ at an O$_2$ partial pressure of 10^{-2} atm.

is concerned, depending on the conditions under which the refractory is being used. Consider for instance first a situation in which an iron oxide-containing refractory body exposed to air is subject to temperature variations in the interval 1300–1500° C. If pure iron oxide is present, a phase change from hematite to magnetite or reverse will tend to make place every time the temperature cycle passes through 1390° C. If on the other hand the iron oxide phase contains 10 wt.% TiO$_2$, the hexagonal hematite (ss) phase is stable up to 1524° C. in air, and no phase changes will take place in the temperature interval 1300–1500° C. As O$_2$ partial pressure is reduced, the magnetite (ss) phases will increase its stability range relative to that of hematite (ss). This corresponds to a displacement of the two-phase area spinel (ss)+hematite (ss) in Fig. 2 toward lower temperatures as O$_2$ partial pressure is decreased. Although quantitative data are not yet available for the system iron oxide-titanium oxide at lower levels of O$_2$ partial pressures, data for iron oxide permits an estimate of the relations to be expected. The sketch in Fig. 3 illustrates the

situation that may be inferred to prevail where magnetite and hematite coexist at an O_2 partial pressure of approximately 10^{-2} atm. Considering the same temperature range as mentioned above, namely 1300–1500° C., pure iron oxide now remains as the single phase magnetite throughout this range, whereas iron oxide containing 10 wt.% TiO_2 begins to transform from α-R_2O_3 to spinel at 1380° C. Hence at this level of O_2 partial pressure (10^{-2} atm.) the presence of TiO_2 may result in damaging phase transformations that did not occur in the presence of pure iron oxide as a constituent of the refractory body.

In contrast to this stabilization by TiO_2 of the hematite phase, which contains essentially all iron as Fe^{3+}, TiO_2 added to liquid iron oxide stabilizes Fe^{2+} relative to Fe^{3+}. This can be seen by an inspection of the lower half of Fig. 2. The heavy dash curve represents compositions of liquids along the liquidus surface, hence temperature is a variable in addition to composition. Because the decomposition of oxide of Fe^{3+} to the oxide of Fe^{2+} is a strongly endothermic reaction, Fe^{3+} is stabilized relative to Fe^{2+} as temperature as decreased, provided O_2 partial pressure and total composition in terms of ratio TiO_2 to total iron oxide remain constant. The stabilizing effect of TiO_2 on Fe^{2+} becomes apparent by following the curve $a\ b\ c\ d\ e$ in Fig. 2 from point a on the iron oxide join toward e as TiO_2 content increases. The first part of this curve ($a\ b\ c$) is pointing approximately toward the TiO_2 corner of the diagram; such a straight line corresponds to constant Fe^{2+}/Fe^{3+} ratios of the liquids. This situation arises because the compositional effect of TiO_2 shifting the equilibrium towards Fe^{2+}, is balanced by an equal effect in the opposite direction of the decrease in liquidus temperature as TiO_2 is added to iron oxide (see upper part of Fig. 2). As the TiO_2 content reaches approximately 27 wt.%, liquidus temperatures start rising rapidly (see upper half of Fig. 2). This causes a discontinuity in the slope of the isobaric curve at c, the curve c–d bending sharply to the right. The rapid increase in Fe^{2+}/Fe^{3+} ratio of liquids with increasing TiO_2 content at point c is the combined result of increasing liquidus temperature and the compositional effect of TiO_2 on the equilibrium. As the TiO_2 content approaches that of the maximum on the liquidus curve (see upper half of Fig. 2), the effect of temperature dies out, and as the liquidus temperatures decrease with further increase in TiO_2 content, the O_2 isobar swings back towards point d. Here the TiO_2 content is that of the pseudobrookite-rutile "eutectic," and further increase in TiO_2 content causes a very sharp increase in liquidus temperatures. Hence a discontinuity in the slope of the O_2 isobar occurs at point d, the curve bending sharply to the right as TiO_2 content increases beyond this point.

The binary joins between the composition points of the stoichiometric end members have been taken to represent compositions of solid solution

crystals in the three series magnetite-ulvospinel ($FeO \cdot Fe_2O_3$-2FeO $\cdot TiO_2$), hematite-ilmenite (Fe_2O_3-$FeO \cdot TiO_2$) and pseudobrookite (Fe_2O_3 $\cdot TiO_2$-$FeO \cdot 2TiO_2$) in the lower half of Fig. 2. This is an approximation made for the purpose of plotting approximately the conjugation lines giving relations between compositions of crystalline and liquid phases existing together in equilibrium. In the case of the magnetite-ulvospinel solid solution, data are available to indicate that this spinel phase contains less Fe^{2+} than corresponding to the stoichiometric ratio (Darken and Gurry, 1946; Chevallier and Gerard, 1950). Compositions of only two crystalline phases, one from the hematite solid solution and one from the pseudobrookite solid solution field, were determined by chemical analysis in the present investigation. The observed compositions fall reasonably close to the expected joins. In the case of rutile which has dissolved some iron oxide in its structure, the mechanism of substitution is not well known. Work on the system FeO-TiO_2 (to be published) has indicated that both Fe^{2+} and Fe^{3+} ions can be accommodated by the rutile lattice. Therefore, conjugation lines in the region where rutile (ss) is the primary crystalline phase have been drawn to the $FeO \cdot Fe_2O_3$-TiO_2 join.

SUMMARY

Phase equilibria in the system iron oxide-TiO_2 in air ($p_{O_2} = 0.21$ atm.) have been studied by the quenching technique.

The relations are represented by a projection into the join $FeO \cdot Fe_2O_3$-TiO_2 of compositions actually located in the ternary system FeO-Fe_2O_3-TiO_2. Points of intersection between the 0.21 atm. O_2 isobar along the liquidus surface and liquidus univariant lines in the ternary system look like eutectic and peritectic points in the apparently binary diagram which results. The main features of the diagram as well as temperatures and phase assemblages at the "invariant" situations are summarized as follows: Hematite is the stable phase of pure iron oxide up to 1390° C. At this temperature hematite and magnetite coexist in equilibrium in air, while magnetite is the stable phase from this temperature up to the liquidus temperature of 1594° C. Magnetite (ss) is the primary crystalline phase in the composition range 0–12 wt.% TiO_2, with liquidus temperatures decreasing to a minimum of 1524° C. At the latter temperature a "peritectic" situation exists with the following phases present together in equilibrium: Spinel (ss), hematite (ss), liquid, gas ($p_{O_2} = 0.21$ atm.). Hematite (ss) is the primary crystalline phase in the composition range 12–27 wt.% TiO_2. At 1493° C. a "eutectic" situation prevails, characterized by the coexistence in equilibrium of hematite (ss), pseudobrookite (ss), liquid and gas ($p_{O_2} = 0.21$ atm.). Pseudobrookite (ss) is the primary crystalline phase in mixtures between 27 and 58 wt.% TiO_2, with the liquidus temperature reaching a maximum of 1550° C. at 45 wt.% TiO_2.

Pseudobrookite (ss), rutile (ss), a liquid containing 58 wt.% TiO_2 and gas exist together in equilibrium at 1515° C. in another "eutectic" situation. Rutile (ss) is the stable phase in mixtures containing more than 58 wt.% TiO_2, with liquidus temperatures increasing from 1515° C. to the melting point of pure TiO_2, approximately 1830° C.

The most significant result of the studies made at subsolidus temperatures is the marked stabilization of the hematite structure relative to that of magnetite as TiO_2 is added to iron oxide, the equilibrium temperature in air increasing from 1390° C. for the pure iron oxide end member to a maximum of 1524° C. In the liquid, TiO_2 stabilizes Fe^{2+} relative to Fe^{3+}.

REFERENCES

AKIMOTO, S., AND NAGATA, T. (1957), The $TiFe_2O_5$-Ti_2FeO_5 solid solution series: *Nature*, **179,** 37–38.

ANDERSSON, S., COLLÉN, B., KUYLENSTIERNA, U., AND MAGNELLI, A. (1957), Phase analysis studies on the titanium-oxygen system: *Acta Chem. Scand.*, **11,** 1641–1652.

BASTA, E. Z. (1953), Ph.D. Thesis, Bristol.

CHEVALLIER, R., AND GIRARD, J. (1950), Synthèse de titanomagnétites: *Bull. Soc. Chim. France*, **17,** 576–581.

CORRUCCINI, R. J. (1949), Differences between international temperature scales of 1948 and 1927: *J. Research Natl. Bur. Standards*, **43,** 133–136.

COUGLIN, J. P. (1954), Contributions to the data on theoretical metallurgy. XII. Heats and free energies of formation of inorganic oxides: *U. S. Bur. Mines, Washington, D. C.* Bull **542.**

DARKEN, L. S., AND GURRY, R. W. (1945), The system iron-oxygen: I, The wüstite field and related equilibria: *J. Am. Chem. Soc.*, **67,** 1398–1412.

DARKEN, L. S. (1946), The system iron-oxygen. II, Equilibrium and thermodynamics of liquid oxide and other phases: *J. Am. Chem. Soc.*, **68,** 798–816.

DEVRIES, R. C., AND ROY, R. (1954), A phase diagram for the system Ti-TiO_2 constructed from data in the literature: *Bull. Am. Ceram. Soc.*, **33,** 370–372.

ERNST, Th. (1943), Über Schmelzgleichgewichte im System Fe_2O_3-FeO-TiO_2 and Bemerkungen über die Minerale Pseudobrookit und Arizonite: *Z. Angew. Min.*, **4,** 394–409.

JUNKER, E. (1936), Zur Kenntnis des Verhaltens des Titandioxydes beim Erhitzen und seines Verhaltens zu Fe_2O_3, Na_2O und MgO: *Z. Anorg. u. Allg. Chem.*, **228,** 97–111.

KAWAI, N., KUME, S., AND SASAJIMA, S. (1954), Magnetism of rocks and solid phase transformation in ferromagnetic minerals: *Prc. Japan. Acad.*, **30,** 588–593.

MUAN, A. (1955), Phase equilibria in the system FeO-Fe_2O_3-SiO_2: J. Metals, 7, September 1955; *Trans. Am. Inst. Mining Met. Engrs.*, **203,** 965–976.

MUAN, A., AND OSBORN, E. F. (1956), Phase equilibria at liquidus temperatures in the system MgO-FeO-Fe₂O₃-SiO₂: *J. Am. Ceram. Soc.*, **39**, 121–40.

MUAN, A., AND GEE, C. L. (1956), Phase equilibrium studies in the system iron oxide-Al₂O₃ in air and at 1 atm. O₂ pressure: *J. Am. Ceram. Soc.*, **39**, 207–214.

MUAN, A. (1957), Phase equilibria at liquidus temperatures in the system iron oxide-Al₂O₃-SiO₂ in air atmosphere: *J. Am. Ceram. Soc.*, **40**, 121–133.

MUAN, A. (1958), Phase equilibria at high temperatures in oxide systems involving changes in oxidation states: *Am. J. Sc.*, **256**, 171–207.

NICHOLLS, G. P. (1955), The mineralogy of rock magnetism: *Advanc. Physics*, **4**, 113–190.

OSBORN, E. F. (1956), Importance of the Spinel Phase in the Steel Industry, pp. 135–150 of *"Regional Technical Meetings," American Iron and Steel Institute, New York*.

PHILLIPS, B., AND MUAN, A. (1958), Phase equilibria in the system CaO-Iron Oxide in air and at 1 atm. O₂ pressure: *J. Am. Ceram. Soc.*, **41**, 445–454.

POSNJAK, E., AND BARTH, T. F. W. (1934), Notes on some structures of the ilmenite type: *Zeit. Krist.*, **88**, 271–280.

POUILLARD, E. (1950), Sur le comportement de l'alumine et l'oxyde de titane vis-a-vis des oxydes de fer: *Ann. de Chim.*, **5**, 164–214.

RAMDOHR, P. (1926), Beobachtungen an Magnetit, Ilmenit, Eisenglanz und Ueberlegungen über das System FeO, Fe₂O₃, TiO₂: *Neues Jahrb. Min., Abt. A, Beil.-Bd.*, **54**, 320–379.

RAMDOHR, P. (1950), Die Erzmineralien und ihre Verwachsungen: Akademie Verlag. Berlin.

RAMDOHR, P. (1953), Ulvospinel and its significance in titaniferous iron ores: *Econ. Geol.*, **48**, 677–687.

SOSMAN, R. B. (1952), Temperature scales and silicate research: *Am. J. Sc.*, **Bowen Volume**, Part 2, 517–528.

VINCENT, E. A., AND WRIGHT, J. B. (1957), Heating experiments on some natural titaniferous magnetites: *Min. Mag.*, **31**, 624–688.

VINCENT, E. A., AND PHILLIPS, R. (1954), Iron titanium minerals in layered gabbros of the Skaergaard intrusion, East Greenland: *Geochim. Cosmochim. Acta*, **6**, 1–26.